Thermodynamic Analysis of Capillary Flows in the Presence of Hydrodynamic Slip

A. Laouir
Dept. of Mechanical Engineering, University of Jijel, BP 98, 18000 Jijel, Algeria

D. Tondeur
Laboratoire des Sciences du Génie Chimique LSGC, BP 451, 54001 Nancy, France

DOI 10.1002/aic.12431
Published online November 2, 2010 in Wiley Online Library (wileyonlinelibrary.com).

A thermodynamic description of liquid flows in capillaries with hydrodynamic slip at the solid–liquid interface is given. Slip over the capillary wall brings into play surface interactions and therefore involves interfacial energy and entropy. Energy and entropy balance equations are written so as to take into account surface effects. The two relations constitute a general mathematical model that allows readily analyzing various situations and to explore the behavior of such thermodynamic process. The main result derived concerns the existence of a capillary pressure of slip; slip occurrence leads to a pressure decrease in the flow and might cause cavitation. The variation in magnitude of the slip effect, viewed as a thermodynamic transformation, may take place irreversibly. Slip irreversibility and the probable occurrence of a two-phase flow regime are possible factors that may cause additional pressure drop. © 2010 American Institute of Chemical Engineers *AIChE J,* 57: 2251–2263, 2011
Keywords: microfluidics, thermodynamics, porous media, surface phenomena, hydrodynamic slip

Introduction

Pressure-driven flow in confined spaces of micrometric and nanometric sizes is the subject of interests in many engineering areas (e.g., microtechnology/nanotechnology, ultrafiltration/nanofiltration, water, and crude oil transport in soils and porous rocks). The possible occurrence of hydrodynamic slip at the solid–liquid interface renders the problem much more complex and invalidates usual prediction methods based on the classical assumption of zero velocity at the solid–liquid interface. The slip phenomenon is at present an area of intense fundamental research covering experimental, modeling, and dynamic molecular simulation aspects. From the practical point of view, the advantage sought is mainly to make certain processes more efficient thanks to friction reduction.[1,2] This aspect is of prime importance when considering for example thermodynamic machines based on surface energy.[3] The prediction of slip and the related quantitative aspects is still a difficult and unresolved problem; moreover, the mechanisms that control it and the physical phenomena involved are not well understood. Experimental works suffer from a certain inadequacy of the theoretical basis generally considered and the results published show important discrepancies.[4–6]

The pressure drop method is an experimental technique used to investigate hydrodynamic slip; the method is indirect and consists in measuring flow rate and pressure drop of a liquid flowing through a capillary, data from which slip magnitude is inferred. The capillary is generally of rectangular or circular cross section.[7–13] Figure 1 represents the aspect of the velocity profile in a circular capillary with slip condition at the solid–liquid interface. In such situation, the fluid

Correspondence concerning this article should be addressed to A. Laouir at ahmed_adr@yahoo.fr.

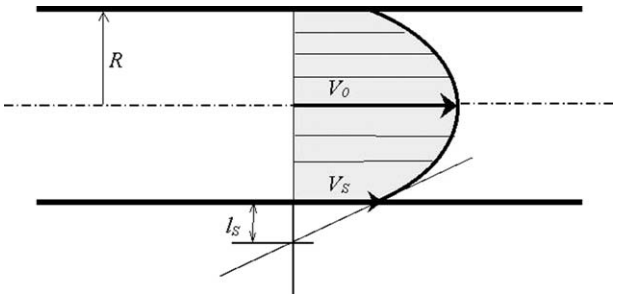

Figure 1. Laminar flow with non-zero velocity at the boundary.

does not stick to the capillary wall as classically assumed at macroscale but slips over the solid with a finite speed V_s. The slip is classically characterized by the slip length l_s defined from the relation,

$$\left.\frac{dV_r}{dr}\right|_R = -\frac{V_s}{l_s} \tag{1}$$

where V_r is the velocity as a function of radius r. Evidence of slip was also shown by an alternative method in which a thin layer of liquid is squeezed between two solid surfaces, one at least being curved.[14,15] Tretheway and Meinhart[16] performed direct measurement of velocity profile and slip velocity near the wall inside a microchannel using micron-resolution particle image velocimetry. Slip lengths reported using different experimental methods range from a few tens of nanometers to a few micrometers. Recent experiments[17,18] performed through carbon nanotube membranes result in l_s values as large as 1.4 μm. In such situation, the velocity distribution is practically uniform, and the process shows nearly a slug flow behavior. Although a reduction in pressure drop is a priori achievable in the presence of hydrodynamic slip, a number of experimental investigations performed with liquids showed an opposite behavior, namely, an increase in pressure drop was observed.[5,6] This unexplained effect arises more noticeably in small size capillaries. Similar unexpected situations were reported by Hasegawa et al.[19] who considered small orifices in place of capillaries.

In this article, a phenomenological thermodynamic approach is considered to study certain consequences of slip occurrence in capillary flows. We show how slip brings into play surface effects, then we apply the first and the second law of thermodynamics so as to include surface energy and entropy. Using a thermodynamic approach, we first analyze reversible situations to highlight some new aspects. Then irreversible flows including friction are treated and the corresponding irreversible pressure drop analyzed.

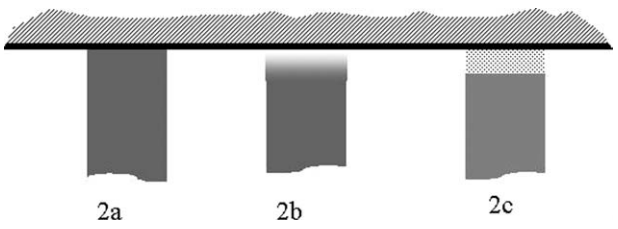

Figure 2. Fluid structure in the vicinity of the capillary wall.

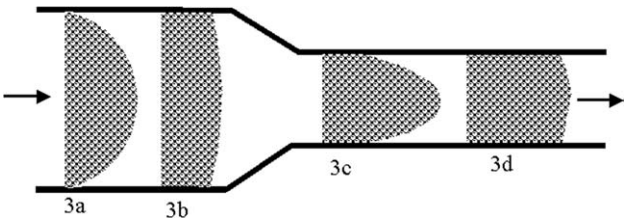

Figure 3. Steady-state slip flow in a capillary.

Slip and Induced Surface Effects

To understand causes and mechanisms of slip, the physical situation prevailing at the boundary has been and remains a subject of controversial discussions. Figure 2 summarizes the hypotheses generally advocated[5,20–23]; in Figure 2a, the slip occurs directly between the liquid and the solid surface and is termed molecular or intrinsic slip. According to certain theoretical analyses, this model fails to explain the strong slip lengths[22] measured in certain experimental works. In Figure 2b, a depletion zone exists between bulk liquid and solid surface; in this layer, the fluid shows important changes in physical properties as compared with those of the bulk. In Figure 2c, a gap is formed between the wall and the liquid by vapor or dissolved gases. From the point of view interesting this work, the situations described above show a certain similarity: The boundary can be considered as a surface (possibly of finite thickness) separating the bulk liquid from the solid, moving with a finite speed V_s and characterized by a finite value of surface tension σ_b.

To point out how surface phenomena may be involved in the presence of hydrodynamic slip in a simple way, one may analyze the process at the molecular scale. Let us reason by considering the intrinsic slip case. In the absence of slip, molecules in contact with the inner surface of the capillary are immobile and this layer sticking to the tube wall prevents other molecules from coming into contact with the tube. The molecules moving in the bulk liquid remain all the time surrounded by other liquid molecules. When the flow gives rise to slip, molecules at the boundary become mobile which renders a possible transfer between the interface and the bulk. At a given cross section of the capillary and for a fixed time interval, the number of molecules in contact with the solid and slipping over it depends on the perimeter and the slip velocity. Variation of one of these two parameters during the flow will modify the number of molecules present at the boundary and cause a transfer between the boundary and the liquid. This transfer constitutes a change in the thermodynamic state and demonstrates that the process involves surface phenomena. This is illustrated in Figure 3, where the spheres symbolize molecules, the number of which is the same in the four situations Figures 3a–d, to represent a steady regime. Figure 3a corresponds to the no-slip regime for which the number of slipping molecules at the boundary is zero. In Figure 3b, the slip occurs, and a finite number of molecules is transferred from the liquid volume to the boundary; the velocity profile is less curved. In Figure 3c,

the slip velocity is equal to that of Figure 3b but the reduction in capillary diameter (and perimeter) forces some molecules to return back to the bulk liquid. In Figure 3d, an increase in slip velocity favors again a transfer from the liquid to the solid–liquid interface.

Quantitatively, for a time interval dt the fluid at the boundary slips along a distance $dx = V_s dt$ and over a surface $dA = P_m dx$ where P_m is the local perimeter at the capillary section considered. The corresponding mass of liquid flowing is $dm = \rho A_c V dt$ where ρ is the liquid density, A_c the local cross-sectional area, and V the mean flow velocity. Per unit mass, the peripheral surface "swept" which we shall call the specific area of slip is $\boldsymbol{a = dA/dm} = \frac{P_m V_s}{\rho A_c V}$, thus for a circular capillary of radius R,

$$a = \frac{2}{\rho R} w \qquad [\mathrm{m}^2.\mathrm{kg}^{-1}] \tag{2}$$

For noncircular capillaries, the hydraulic radius $R_H = 2A_c/P_m$ is to be considered. In the following, we shall consider circular capillaries, relations specific to rectangular channels are summarized in Appendix C. The ratio $w = V_s/V$ is a nondimensional quantity convenient to characterize the slip rate; for the non-slip condition, we have $w = 0$ and for maximum slip, $w = 1$. The quantity w may be expressed as a function of the slip length l_s and the capillary radius if the velocity profile is known (see Appendix A, Eq. A7 for laminar flow). The quantity a defined by Eq. 2 may be expressed as a function of the volume flow rate $\dot{v} = V\pi R^2$,

$$a = \frac{2\pi R}{\rho} \frac{V_s}{\dot{v}} \tag{2'}$$

Physically, the quantities (R,w) in Eq. 2 and ($\dot{v}$,R, V_s) in Eq. 2′ are not independent. The knowledge of the mathematical expressions relating them and possibly to other physical properties of the liquid and the interface is an important issue as it allows predicting quantitatively the slip. Unfortunately, this problem is not yet resolved, although in this perspective molecular dynamics simulation is intensively used as an investigation tool.[24–28] As stated in the introduction, we are concerned with the analysis of the consequences of hydrodynamic slip assuming that the conditions of its occurrence are fulfilled, and in the absence of a predictive model, the parameter w is regarded as an independent parameter.

In the light of the mechanism described above, it appears that the knowledge of the surface tension at the interface between the bulk liquid and the capillary wall σ_b is of prime importance to develop a thermodynamic description of a slip flow. According to the models of Figure 2, in the presence of a gas gap, we can reasonably assume $\sigma_b = \sigma_{lv}$; for intrinsic slip, one may assume $\sigma_b \approx \sigma_{sl}$ although there is no proof that a solid–liquid interface with wall slip is equivalent to a static solid–liquid interface with the same value of interfacial tension. The case of intrinsic slip shows peculiar feature in so far as it leads to a continuous change of the area of the solid–liquid interface. This process is equivalent to a pseudo elastic extension/contraction of the (sl) interface, an experiment which is impossible to perform in a batch process because of the solid rigidity. For this reason, it cannot be identified with one of the known situations described in textbooks on surface phenomena, namely wetting, adhesion, and spreading processes.[29,30] Slip with gas gap is simply an elastic extension/contraction of the (lv) surface as classily experienced but performed here in a continuous manner. What may be pointed out is that hydrodynamic slip may offer an opportunity to bring into play surface phenomena in continuous steady state processes and to take advantage of the associated energy. This is conceivable providing the slip results at the same time in a substantial reduction in friction losses compared with nonslip Poiseuille flow.

Surface Energy and Surface Entropy

The internal energy and entropy per unit area associated to a surface or an interface separating two phases are given by,[31–33]

$$u_{**} = -T\frac{\partial \sigma_{**}}{\partial T} + \sigma_{**}; \quad S_{**} = -\frac{\partial \sigma_{**}}{\partial T} \tag{3}$$

σ_{**} is the surface tension, and subscript (**) designates the surface type (sl), (lv), or (sv). The free energy is $u_{**} - Ts_{**} = \sigma_{**}$ which means that σ_{**} is the thermodynamic work involved to create isothermally one square meter of interface. Surface tensions are interrelated by Young equation, $\sigma_{sl} = \sigma_{sv} - \sigma_{lv}\cos\theta$, where θ is the contact angle of the solid–liquid couple considered. Liquids in contact with clean high-energy surfaces like hard inorganic solids (e.g., metals, glass, silicon…) will spread[34] and show small and even zero value contact angle θ. For usual liquids, σ_{lv} is lower than 80×10^{-3} J m^{-2}, whereas for high-energy solids σ_{sv} exceeds 1 J m^{-2}; in this situation $\sigma_{sl} \gg \sigma_{lv}$. Low-energy surfaces are represented by solid organic compounds, in this case σ_{sv}, σ_{lv}, and σ_{sl} are of the same order of magnitude and the contact angle has a finite positive value. A high-energy surface may be treated to decrease its surface energy and thus lower its wettability by depositing a thin layer of an appropriate organic compound.

From the experimental point of view only σ_{lv} and θ are directly measurable. An important aspect concerns the problem of calculating σ_{sl} and σ_{sv} from experimental values of σ_{lv} and θ. Mathematically, a second relation involving σ_{sl} and σ_{sv} is needed in addition to Young's equation. This theoretical problem is not yet completely resolved. Specifically for low-energy surfaces,[35] a semi-empirical relation was proposed.[36,37] Table 1 gives surface properties of some solid–liquid systems (the solids are of low-energy type); the values of σ_{lv}, θ, and the derivatives $\partial\sigma_{lv}/\partial T$, $\partial\theta/\partial T$ are from experimental measurements, the other quantities relative to (sv) and (sl) surfaces are inferred according to Neumann's method.[36]

Energy and Entropy Balance

As we are concerned with slip flows in capillaries, it is of importance to define the overall enthalpy h_g of the liquid so as to incorporate surface effects. This question will be considered in a more general form than was done in a previous work,[38] the validity of which was restricted to total intrinsic slip ($w = 1$) with the approximation $\sigma_{sl} \approx -\sigma_{lv}\cos\theta$ (low-energy surface with a high-surface tension liquid). The overall enthalpy h_g in presence of hydrodynamic slip is the sum

Table 1. Surface Properties of Some Solid/Liquid Systems at 293.15 K (20°C) considered by Neumann[36]

Solid/Liquid System	σ^*_{lv}	θ^*	σ_{sv}	σ_{sl}	$\frac{\partial\sigma^*_{lv}}{\partial T}$	$\frac{\partial\theta^*}{\partial T}$	$\frac{\partial\sigma_{sv}}{\partial T}$	$\frac{\partial\sigma_{sl}}{\partial T}$
Siliconed glass/water	72.8	1.870	18.3	39.83	−0.16	$+8.5 \times 10^{-4}$	−0.126	−0.141
Siliconed glass/decane	23.9	0.248	23.2	0.03	−0.092	-25.5×10^{-4}	−0.084	0.005
Cholesteryl acetate/water	72.8	1.804	21.0	37.87	−0.16	-2.1×10^{-4}	−0.085	−0.130

Units are mJ m^{-2}, mJ m^{-2} K^{-1}, Rad, and Rad K^{-1}.
"*" designates experimental value.

of the usual bulk liquid enthalpy $h_l = u_l + Pv_1$ and the local interfacial energy given by the product $u_b a$,

$$h_g = h_l + u_b a \tag{4}$$

likewise the overall entropy is,

$$s_g = s_l + s_b a \tag{5}$$

u_b and s_b are given by Eq. 3 in units of J m^{-2} and J m^{-2} K^{-1}, respectively, so that the products $u_b a$ and $s_b a$ have the dimensions of J kg^{-1} and J kg^{-1} K^{-1}, respectively. From Eqs. 4 and 5, one may note that the quantity a constitutes a thermodynamic coordinate that determines, with temperature, pressure, and specific volume, the thermodynamic state of a liquid undergoing a slip flow. Thus, processes involving variations of the quantity a constitute in fact thermodynamic transformations. For a steady state flow, the general form of energy balance equation written for a given control volume is,

$$\dot{Q} + \dot{W} + \sum \dot{m}(h_g + e_c + e_p) = 0 \tag{6}$$

$\dot{Q}$ is the rate of heat transfer, $\dot{W}$ is the mechanical energy transfer, e_c and e_p are specific kinetic and potential energies related to the flow stream $\dot{m}$. The entropy balance equation is,

$$\frac{\dot{Q}}{T} + \sum \dot{m} s_g + \dot{\varepsilon} = 0 \tag{7}$$

where $\dot{\varepsilon}$ the entropy production rate which is zero for a reversible process, and the summation applies algebraically to inlet and outlet flows of the control volume. Actual processes may be brought close to reversibility in principle when they are performed at sufficiently slow rates, this also requires in general an appropriate design of the system in which the process takes place. The application of the first and the second law of thermodynamics to various situations involving surface phenomena was previously considered in a general paper,[39] this study is another contribution leaning on the ideas presented in that work.

Figure 4 sketches the system, in two forms that correspond to the problem interesting this study. The capillary may be one or many placed in parallel as encountered with membranes. No work is involved in such problem, only heat may be transferred from or to the system. In general case than represented in Figure 4, potential energy variation may be significant. Per unit mass of liquid, Eqs. 6 and 7 simplify to the forms,

$$Q + \left(h_g + \frac{1}{2}V^2 + gz\right)_1 - \left(h_g + \frac{1}{2}V^2 + gz\right)_2 = 0 \tag{8}$$

$$\frac{Q}{T} + s_{g1} - s_{g2} + \varepsilon = 0 \tag{9}$$

where the subscripts 1 and 2 refer to the inlet and outlet of the section considered.

Reversible and Isothermal Flow

The flow is performed at constant temperature T and assumed free from friction, an idealized situation analogous to the one considered when establishing the Bernoulli equation, and introduced here to focus attention upon some peculiar features concerning slip. Eliminating Q from Eqs. 8 and 9 and substituting h_g and s_g by their expressions (Eqs. 4 and 5) and letting $\varepsilon = 0$,

$$\Delta h_l - T\Delta s_l - \Delta(a\sigma_b) + 1/2\Delta V^2 + g\Delta z = 0 \tag{10}$$

for the liquid $dh_1 - Tds_1 = v_1 dP$, assuming the liquid of constant density $\rho = 1/v_1$, the integration gives $\Delta h_1 - T\Delta s_1 = \Delta P/\rho$; Eq. 10 may be written,

$$\frac{P}{\rho} + \frac{1}{2}V^2 + gz + \frac{2w}{\rho R}\sigma_b = cste \tag{11}$$

Equation 11 may be considered as an extended form of the classical Bernoulli equation that takes into account the surface energy. Considering the pressure variation, this relation may be rewritten:

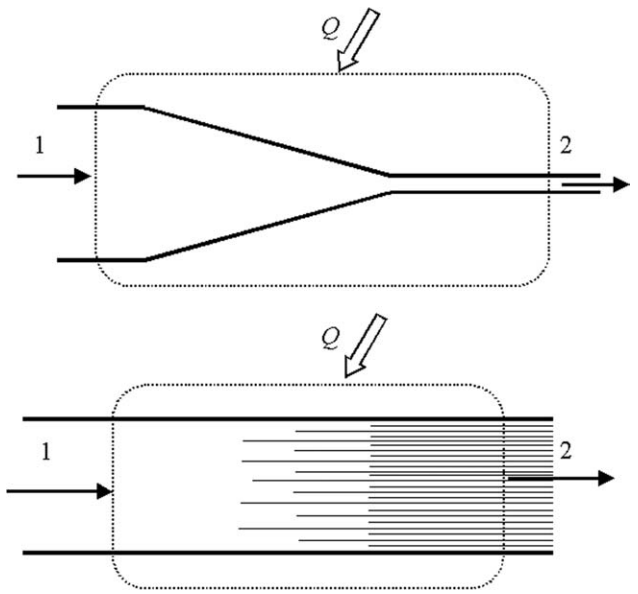

Figure 4. Pressure driven flow through a capillary or capillaries in parallel.

Table 2. Capillary Pressure of Slip and Heat Transferred for Isothermal Flow at 293.15 K (20°C) Calculated According to Eqs. 14 and 16

Solid/Liquid System	Capillary Radius R (μm)	Slip over a Gas Gap $\sigma_b = \sigma_{lv}$		Intrinsic Slip $\sigma_b = \sigma_{sl}$	
		$\frac{\Delta P_\sigma}{w}$ (Pa)	$\frac{Q}{w}$ (J kg^{-1})	$\frac{\Delta P_\sigma}{w}$ (Pa)	$\frac{Q}{w}$ (J kg^{-1})
Siliconed glass/water	5	-0.3×10^5	18.8	-0.2×10^5	16.5
	0.5	-2.9×10^5	187.8	-1.6×10^5	165.5
	0.005	-291.0×10^5	18,780.4	-159.0×10^5	16,550.2
Siliconed glass/decane	5	-0.1×10^5	14.9	0.0×10^5	-0.8
	0.5	-1.0×10^5	149.0	0.0×10^5	-8.1
	0.005	-96.0×10^5	14,900.4	0.0×10^5	-809.8
Cholesteryl acetate/water	5	-0.3×10^5	18.8	-0.1×10^5	15.3
	0.5	-2.9×10^5	187.8	-1.5×10^5	152.6
	0.005	-291.0×10^5	18,780.4	-151.0×10^5	15,259.1

A dimensional parameter w is the slip rate ($0 \leq w \leq 1$).

$$\Delta P = -\frac{\rho}{2}\Delta V^2 - \rho g \Delta z - 2\Delta\left(\sigma_b \frac{w}{R}\right) = \Delta P_V + \Delta P_z + \Delta P_\sigma \tag{12}$$

where $\Delta P \equiv P_2 - P_1$. Equation 12 shows that slip occurrence causes a supplementary pressure variation ΔP_σ in addition to those related to velocity and elevation changes ΔP_V and ΔP_z, respectively. If the nature of the interface is the same at both states 1 and 2, that is, $\sigma_{b1} = \sigma_{b2} = \sigma_b$, then:

$$\Delta P_\sigma = -2\left(\frac{w_2}{R_2} - \frac{w_1}{R_1}\right)\sigma_b(T) \tag{13}$$

ΔP_σ is a new form of capillary pressure related to hydrodynamic slip. It is different from the known capillary pressure of wetting given by the Washburn-Laplace equation $\Delta P = 2\sigma_{lv}\cos\theta\Delta(1/R)$. The latter concerns situations where a "dry" surface of a solid is to be wetted by a liquid and occurs even at static state. Capillary pressure of slip Eq. 13 is related to liquid displacement and vanishes when the flow is stopped. Pressure variations caused by slip, taken alone, in the flow represented in Figure 3 can now be discussed using Eq. 13 (for convenience w/R may be replaced by $\pi R V_s/\dot{v}$); one could check that $P_{3a} > P_{3b} < P_{3c} > P_{3d}$.

Forced passage of a liquid from a large tube into a capillary corresponds to a situation where $R_1 \gg R_2$ and consists of a transition from no-slip to slip state, that is $w_1 = 0$ and $w_2 \neq 0$. Letting $w = w_2$ and $R = R_2$, Eq. 13 reduces to,

$$\Delta P_\sigma = -\frac{2w}{R}\sigma_b(T) \tag{14}$$

a negative quantity, showing that slip development in the capillary causes a decrease in pressure. This is consistent with the fact that to create more interface, namely to increase the quantity a, involves an expense of a certain amount of thermodynamic work given here by the work of pressure forces. The process involves heat Q, which may be calculated from entropy balance Eq. 9,

$$Q = T(s_{l2} - s_{l1}) - 2T\frac{\partial\sigma_b}{\partial T}\left(\frac{w_2}{\rho_2 R_2} - \frac{w_1}{\rho_1 R_1}\right) \tag{15}$$

The term $T(s_{l2} - s_{l1})$ is the heat associated to the liquid compressibility (which vanishes if the fluid is assumed incompressible), the remaining term is the heat associated to surface interactions involved by slip. If $R_1 \gg R_2$ (or $w_1 = 0$), and assuming incompressibility:

$$Q = -2\frac{T}{\rho}\frac{w}{R}\frac{\partial\sigma_b}{\partial T} \tag{16}$$

This relation shows that the process is endothermal if $\partial\sigma_b/\partial T < 0$; this is systematically true in the case of a (lv) surface of a pure liquid ($\sigma_b = \sigma_{lv}$); but no general rule may be given in the case of a (sl) interface ($\sigma_b = \sigma_{sl}$). Table 2 gives numerical values of ΔP_σ and Q associated to slip flows according to Eqs. 14 and 16, slip rate w is left as a parameter. The values are calculated for three capillary sizes in a zone where surface effects are significant. The minimum value of R is 5×10^{-9} m, under this limit surface tension values are significantly affected.[31,40] Pressure decrease due to slip may be dramatically high for small size capillaries, and this is true as long as slip is significant, thus for w not too small. Heat values show that the process is endothermal except for intrinsic slip with siliconed glass/decane system. This pair shows a positive sign of $\partial\sigma_{sl}/\partial T$ explaining this behavior. Heat exchange per kg of liquid is generally small but becomes noticeable in very thin capillaries. The most elevated heat value is 18.78×10^3 J kg^{-1} with water in 5×10^{-9} m radius capillary (for a perfect slip, $w = 1$). Slip effects may be much more elevated if intrinsic slip over high-energy surfaces is considered. As explained in a previous paragraph, for these solids σ_{sl} values may be extremely high.

The strong decrease in pressure inside the capillary when slip takes place is a remarkable feature that should retain the attention. Indeed an important drop of the absolute pressure can logically cause the release of dissolved gases and ultimately gives rise to liquid evaporation. Because of capillary smallness the vaporization process will take place at the surface without nucleation in bulk liquid.[41] The development of a gas layer at the boundary increases the slip because of its lubricating role[23]; in turn, the slip amplification causes more pressure decrease according to Eq. 14 and more vapor will be produced. This mechanism could eventually generate cavitation and cause profound disturbance of the hydrodynamics. Mishra and Peles[42,43] have studied cavitation of water past micro-orifices and micro-venturis, they reported certain deviations from the macroscale results and explained that surface effects may be a probable cause. From the discussion exposed in this paragraph, it follows that cavitation at microscale may be initiated and maintained by the slip as the

latter contributes to the pressure decrease in addition to inertial effects related to velocity. The experiments of Mishra and Peles probably involved hydrodynamic slip, which may explain the deviations observed.

Another aspect to analyze concerns the vapor pressure in the gap separating the liquid and the capillary. It is well established[31] that the curvature of the (lv) surface creates a difference between the liquid pressure P_2 and the vapor pressure P_{gap} given by,

$$P_{\text{gap}} - P_2 = -\frac{2}{R}\sigma_{\text{lv}} \tag{17}$$

On the other hand, the curvature causes an increase in vapor tension P^{sat} according to Kelvin relation,

$$\ln\left(\frac{p^{\text{sat}}}{P_0^{\text{sat}}}\right) = \frac{2\sigma_{\text{lv}}}{\rho R}\frac{M10^{-3}}{R_{\text{id}}T} \tag{18}$$

P_0^{sat} is the saturation pressure for noncurved surface ($R \to \infty$), M is the molar mass, and R_{id} is the ideal gas constant. In the gap $P_{gap} = P^{\text{sat}}$ and $P^{\text{sat}} > P_0^{\text{sat}}$ which signifies that the vaporization process is facilitated by the curvature, this fact constitutes a supplementary factor favoring vapor phase occurrence during the flow particularly at submicrometric scale (to give an idea, for $R = 0.5 \times 10^{-6}$ m, $P^{\text{sat}}/P_0^{\text{sat}} \approx 1$ with most liquids and for $R = 5 \times 10^{-9}$ m, $P^{\text{sat}}/P_0^{\text{sat}} = 1.24$ with water and 2.16 with decane). Combining Eqs. 14 and 17, the pressure in the gap can be related to the external driving pressure P_1,

$$P_{\text{gap}} = P_1 - \frac{2}{R}(1 + w_2)\sigma_{\text{lv}} \tag{19}$$

Equation 19 shows that the pressure in the gap is the consequence of the longitudinal (streamwise) pressure decrease because of the slip and the radial pressure decrease due to the curvature of the (lv) surface. In writing Eq. 19, the gap dimension is supposed negligible compared with capillary radius.

The previous discussion permits to notice that the hydrodynamic slip by itself highly favors the occurrence of an annular gaseous space between the liquid and the wall. One may conclude that for very thin capillaries, slip with a rarefied gas gap is the situation that will prevail. If the liquid contains dissolved gases they will be liberated earlier at more elevated values of P_{gap}. This is consistent with experimental results showing that on the one hand the slip takes place more easily in small size capillaries, Holt et al.[18] observed huge slip of water in carbon nanotubes, on the other the presence of dissolved gases in the liquid facilitates its occurrence.[1] If we assume that the gas gap existence at the boundary is simply a vapor–liquid equilibrium problem, Eqs. 18 and 19 gives the conditions leading to its occurrence. A complete discussion about this aspect should take into account pressure drop due to friction set aside here as we have considered a reversible process (see Appendix B in relation with the section entitled Pressure Drop in Viscous Flow Involving Slip Irreversibility).

Reversible and Adiabatic (Isentropic) Flow

In this section, we consider the flow as adiabatic ($Q = 0$) and reversible ($\varepsilon = 0$) so that the overall entropy s_g remains constant. Ignoring the mass of the solid and considering the thermodynamic system as only composed of the liquid and the surface, Eqs. 8 and 9 take the respective forms:

$$s_l - \frac{\partial\sigma_b}{\sigma T}a = cste \tag{20}$$

$$h_{\text{l}} + \left[\sigma_{\text{b}} - T\frac{\partial\sigma_{\text{b}}}{\partial T}\right]a + gz + \frac{1}{2}V^2 = cste \tag{21}$$

These equations govern the process for which both T and P vary. This set of two equations is nonlinear so it normally has to be solved iteratively. For an incompressible liquid having a heat capacity c_v, we have $h_1 = c_vT + P/\rho$ and $s_1 = c_v \ln T$. Neglecting kinetic and potential energies and considering $R_1 \gg R_2 = R$, the temperature T_2 may be calculated from the entropy balance Eq. 20,

$$c_{\text{v}} \ln T_2 - \left[\frac{\partial\sigma_{\text{b}}}{\partial T}a\right]_2 = c_{\text{v}} \ln T_1 \tag{22}$$

where $\partial\sigma_b/\partial T$ is a function of T_2. For linear variations of $\sigma_b = \sigma_b(T)$ or for small temperature variations between the states 1 and 2, $\partial\sigma_b/\partial T$ can be taken constant, thus resolving for T_2 yields:

$$T_2 = T_1 \exp\left(\frac{a_2}{c_{\text{v}}}\frac{\partial\sigma_{\text{b}}}{\partial T}\right) \tag{23}$$

Generally, we have $\left|\frac{a_2}{c_v}\frac{\partial\sigma}{\partial T}\right| << 1$ so that the following approximation may be adopted:

$$\frac{T_2}{T_1} \approx \left(1 + \frac{2}{\rho c_{\text{v}}}\frac{w}{R}\frac{\partial\sigma_{\text{b}}}{\partial T}\right) \tag{24}$$

This relation shows that for the general case where $\partial\sigma_b/\partial T < 0$, the slip causes a decrease in temperature and vice versa. Values of T_2/T_1 calculated for water ($\rho = 999$ kg m^{-3}; $c_v = 4185$ J kg^{-1} K^{-1}) and for decane ($\rho = 724$ kg m^{-3}; $c_v = 2213$ J kg^{-1} K^{-1}) are about 0.98 with $R = 5 \times 10^{-9}$ m for a perfect slip ($w = 1$). That is, in the extreme case, the temperature changes from 293.15 K to about 287 K. This result shows that, at least with usual fluids and low-energy surfaces, the temperature variation in the adiabatic process is not significant. In addition, the mass of the solid ignored in this analysis acts as a heat reservoir and further mitigates the temperature variation.

The pressure difference may be calculated from Eq. 21,

$$P_2 - P_1 = -\rho\left[\sigma_{\text{b}}(T_2) - T_2\frac{\partial\sigma_{\text{b}}}{\partial T}\right]a_2 - \rho c_{\text{v}}(T_2 - T_1) \tag{25}$$

using Eq. 24 and noting that for a constant $\partial\sigma_b/\partial T$, the internal energy u_b is constant,

$$\sigma_{\text{b}}(T_2) - T_2\frac{\partial\sigma_{\text{b}}}{\partial T} = \sigma_{\text{b}}(T_1) - T_1\frac{\partial\sigma_{\text{b}}}{\partial T} \tag{26}$$

finally,

$$\Delta P_\sigma = -\frac{2w}{R}\sigma_{\text{b}}(T_1) \tag{27}$$

a relation similar to Eq. 14, which shows that the temperature change (negligible or not) in an adiabatic slip flow does not affect the pressure difference; the process behaves as if it was performed at constant temperature T_1. As a conclusion, according to the comments done about Eqs. 24 and 27, a slip flow is rather isothermal unless heated or cooled from the outside.

On the Irreversibility of Slip and Geometric Changes

Slip development and variation in magnitude and mode according to the boundary type is a thermodynamic process that modifies the energy and the entropy of the thermodynamic system consisting of the liquid and the surface. The question that arises is how this kind of process may become irreversible, in other words what are the circumstances that may compromise the thermodynamic reversibility of a slip flow and what are the consequences. As we are considering an unfamiliar process, in an attempt to develop a coherent analysis both formal and qualitative aspects will be combined. Formally, for an irreversible process, the entropy production ε is strictly positive in Eq. 9. Doing the same as was done for the reversible isothermal flow and resolving for ΔP, we obtain:

$$\Delta P = -\frac{\rho}{2}\Delta V^2 - \rho g \Delta z - 2\Delta\left(\frac{w}{R}\sigma_b\right) - T\rho\varepsilon \qquad (28)$$

or,

$$\Delta P = \Delta P_V + \Delta P_z + \Delta P_\sigma + \Delta P^\varepsilon \qquad (28')$$

the heat Q transferred is derived from the entropy balance equation; for an uncompressible fluid,

$$Q = -\frac{2}{\rho}T\Delta\left(\frac{\partial\sigma_b}{\partial T}\frac{w}{R}\right) - T\varepsilon \qquad (29)$$

$\Delta P^\varepsilon = -T\rho\varepsilon$ is the irreversible pressure drop related to the entropy generation and $-T\varepsilon$ the corresponding heat rejected. ΔP^ε is always negative, whereas ΔP_σ, ΔP_V, and ΔP_z are reversible pressure variations, positive or negative.

In this section, we shall again consider the flow as nonviscous and the possible entropy generation is then only caused by transformations involving variation of slip. The possible irreversible behavior of the slip under certain conditions is a remarkable aspect to analyze as it will result in a particular contribution to pressure drop $\Delta P^\varepsilon = \Delta P^\varepsilon_\sigma$ unknown at macroscale.

In the previous sections, the thermodynamic reversibility was assumed to derive Eq. 13. To further analyze, the reversibility in the presence of slip, we consider the differential form of Eq. 13,

$$dP_\sigma(x) = -2\sigma_b d\left(\frac{w(x)}{R(x)}\right) \qquad (30)$$

where x is the longitudinal coordinate (streamwise). Eq. 30 establishes a relation between the geometrical parameter $R(x)$ and the capillary pressure $P_\sigma(x)$ and the slip rate $w(x)$ for an equilibrated process. This also means that to promote thermodynamic reversibility in a slip flow, the process should be performed so that Eq. 30 holds all along the capillary. For example in the case of a uniform capillary of constant radius R, the flow is reversible when $\Delta P_\sigma(x)$ is actually proportional to $\Delta w(x)$ according to the relation $dP_\sigma(x)/dw(x) = -2\sigma_b/R$. Figure 5a represents such a case: $w(x)$ is assumed linear and this imposes that $P_\sigma(x)$ should also be linear. Conversely if $w(x)$ and $P_\sigma(x)$ are known or chosen functions, the capillary should have the appropriate shape $R(x)$ given by the integration of Eq. 30 to insure an equilibrated slip evolution. As exposed in the second section, slip occurrence and development involves displacement of molecules from the bulk liquid to the boundary and vice versa when it diminishes. As a general rule, one could assert that the reversibility is conditioned by orderly and to a certain degree, slow molecules transfer. Slow rate of molecules transfer signifies a progressive and equilibrated change in slip. Experimental observations reported that the slip increases when the radius is reduced, so in practice the speed at which the slip develops may be controlled by controlling the radius variation streamwise, and a convergent tube is the convenient shape for a progressive and equilibrated slip development; a divergent tube for the opposite process. The case of a reversible slip flow in a cylindrical capillary discussed above is rather hypothetical as a constant cross section would not be compatible with an equilibrated slip variation especially at the entrance and exit zones. Figure 5b illustrates schematically the convergent-divergent shape convenient to perform a reversible slip development and disappearance; the pressure difference between the capillary ends is therefore zero.

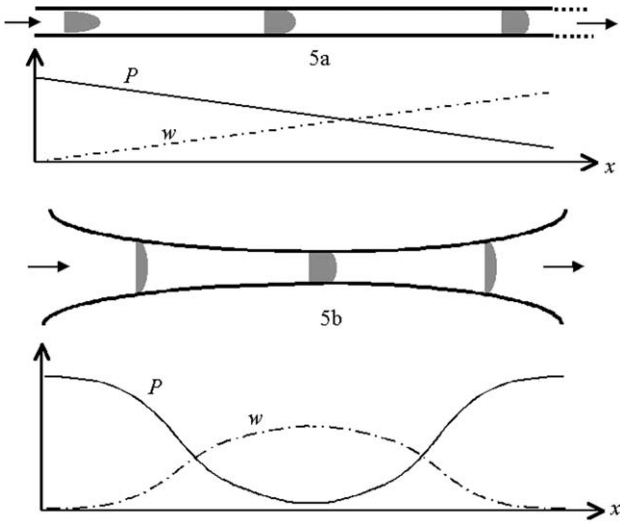

Figure 5. Qualitative variation of pressure and slip rate for a reversible flow in a uniform (a) and a convergent-divergent capillary (b).

Figure 6 describes two situations that may cause slip irreversibility and the qualitative variations of P and w. In Figure 6a, because of an abrupt increase in cross-sectional area the fluid undergoes a nonequilibrated transition from slip to no-slip state. The slipping molecules at the boundary return at once and disorderly to bulk liquid, and this brutal change in state will in principle lead to thermodynamic losses in form of an irreversible pressure drop $\Delta P^\varepsilon_\sigma = P_2 - (P_2)_{rev}$, were P_2 is the actual exit pressure and $(P_2)_{rev}$ the ideal (reversible) pressure, $(P_2)_{rev} = P_1 + \Delta P_\sigma$. This situation is

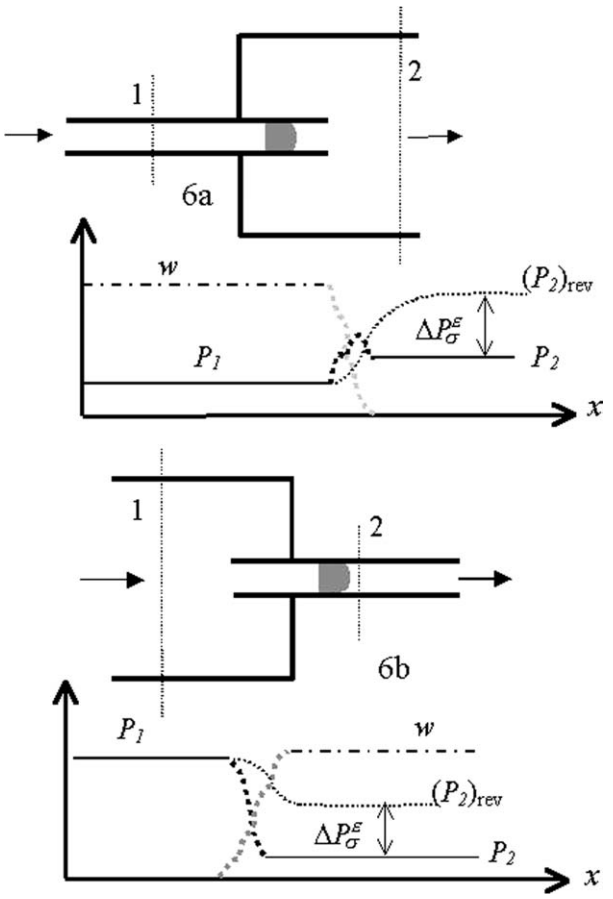

Figure 6. Irreversible slip transition following a sudden disappearance (a) or development (b) of the solid–liquid interface resulting in an irreversible pressure drop $\Delta P_\sigma^\varepsilon$.

similar to that known with bubbles collapsing in liquids; in this case the liquid–vapor surface vanishes also in a brutal manner and the free energy σ_{lv} is destroyed into heat. Figure 6b shows the inverse process, a situation that may occur at the capillary entrance. The irreversible transition from no-slip to slip state results as well in a pressure drop $\Delta P_\sigma^\varepsilon$. To characterize such irreversible processes one may define a thermodynamic efficiency η as follows,

$$\eta = \frac{P_2 - P_1}{\Delta P_\sigma} \text{ for } \Delta P_\sigma > 0 \tag{31}$$

and

$$\eta = \frac{\Delta P_\sigma}{P_2 - P_1} \text{ for } \Delta P_\sigma < 0 \tag{32}$$

the irreversible pressure drops related to slip transition are thus,

$$\Delta P_\sigma^\varepsilon = -(1-\eta)\Delta P_\sigma \text{ for } \Delta P_\sigma > 0 \tag{33}$$

and

$$\Delta P_\sigma^\varepsilon = \left(\frac{1}{\eta} - 1\right)\Delta P_\sigma \text{ for } \Delta P_\sigma < 0 \tag{34}$$

Irreversible processes related to slip variation might also take place inside the capillary if for any reason slip evolution is not equilibrated. In summary, one may conclude that slip as a thermodynamic process may be irreversible and hence could cause a pressure drop. This effect is quite probable as thermodynamic transformations in general have a natural tendency to occur irreversibly. To avoid (or to reduce) this effect, certain precautions should be taken as discussed above.

Pressure Drop in Viscous Flow Involving Slip Irreversibility

In this paragraph, we shall consider the typical situation encountered in the pressure drop method used to investigate hydrodynamic slip. A liquid is forced to flow in a uniform (constant diameter) capillary, the quantities directly measured are the flow rate $\dot{v}$ and the irreversible pressure drop ΔP^ε between the two ends. The key problem in this method is to know exhaustively all the factors contributing to the total pressure drop and to have the corresponding models. In macroscopic and incompressible flows, viscous dissipation is practically the unique factor that causes pressure loss. In small capillaries, many researchers admit the existence of other factors even not well identified. Electro-viscous effect[44,45] may contribute to increase the pressure drop if the liquid contains ions or is polar, but Janssens-Maenhout and Schulenberg[44] have shown that this effect alone cannot explain the unexpected elevated pressure drop observed for example in the work of Hasegawa et al.[19] As analyzed in the previous section, slip variations taking place irreversibly may cause additional pressure drop $\sum \Delta P_\sigma^\varepsilon$. Considering the fluid pure and nonpolar to ignore electro-viscous effects, the total pressure drop is then,

$$\Delta P^\varepsilon = \Delta P_\mu + \sum \Delta P_\sigma^\varepsilon \tag{35}$$

ΔP_μ is the pressure drop related to viscosity μ; for a uniform capillary of length L, its expression is given by Poiseuille relation corrected for slip (see Appendix A),

$$\Delta P_\mu = -8\mu LV(1-w)/R^2 = (1-w)\Delta P_{\mu 0} \tag{36}$$

where $\Delta P_{\mu 0} = -8\mu LV/R^2$ is the pressure drop for the flow without slip. Entrance and exit viscous losses may be neglected in general if $L \gg R$. Figure 7 illustrates the pressure variation in a slip flow of a viscous fluid, for the sake of simplicity, irreversible slip is supposed only caused at the exit. Even if we are not concerned with roughness problems, we mention briefly the related findings. Unlike macroscale flows, at small scale roughness may affect noticeably the flow resistance even in laminar regime by increasing the friction coefficient and the pressure drop.[9,10] The hypothesis of turbulent flow regime occurrence at lower Reynolds numbers is also advocated.[8,9] On the other hand, surfaces with specially designed roughness[2] can show strong apparent hydrophobicity and facilitate slip occurrence.

The slip is intimately linked to the parietal friction at the boundary, the latter controlling both slip occurrence and magnitude.[46,47] Wall-friction may be modeled so as to introduce a friction coefficient[26,47] f giving a friction stress fV_s; the later constitutes the reaction to the viscous shear stress

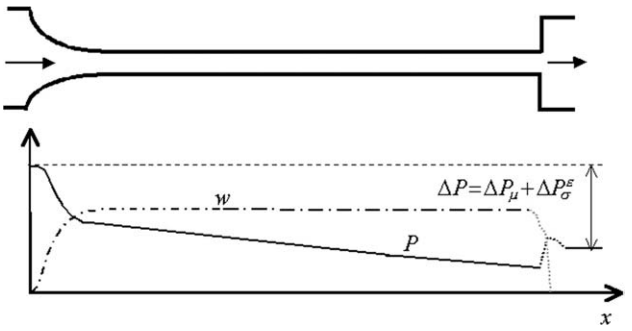

Figure 7. Pressure drop analysis in a cylindrical capillary.

The convergent shape at the entrance insures a reversible slip development. Inside the capillary the pressure decreases linearly due to viscosity. Abrupt change in cross-sectional area at the outlet causes a slip-transition pressure drop $\Delta P_\sigma^\varepsilon$.

$\mu(dV_r/dr)_R$ exerted by the fluid. Algebraically this may be written as $\mu(dV_r/dr)_R + fV_s = 0$. From Eq. 1 one gets $f = \mu/l_s$, and from Eq. A7, the slip length l_s can be expressed as a function of w, as $l_s = Rw/4(1 - w)$ so that finally:

$$f = 4\mu(1 - w)/(wR) \tag{37}$$

Relation (37) shows that the friction coefficient is infinite in the absence of slip ($w = 0$) and vanishes in the case of perfect slip ($w = 1$).

In most experimental works, the measures are analyzed by supposing the pressure drop only caused by viscous dissipation, that is $\Delta P^\varepsilon = \Delta P_\mu$. In doing so, ΔP_μ may be overestimated if in the real facts the measured pressure drop results in part from other effects. This hypothesis finally leads to underestimate the slip magnitude (negative values of slip lengths were found in certain cases attributed generally to measurement errors). In addition to irreversible slip transition, cavitation may constitute another factor that may increase significantly the total pressure drop. As shown in the previous sections, because slip development can strongly lower the pressure, the fluid may easily shift to a two-phase flow regime (this effect is not included in Eq. 35 because we are considering a single-phase flow and the gas gap thickness is small). A slip flow is attractive, inasmuch as it leads to a reduction in the pressure drop if $|\Delta P^\varepsilon| < |\Delta P_{\mu 0}|$. According to Eqs. 35 and 36, this is equivalent to:

$$w\left|\Delta P_{\mu 0}\right| > \sum \left|\Delta P_\sigma^\varepsilon\right| \tag{38}$$

This result brings to the foreground that pressure drop reduction by hydrodynamic slip is not achievable in all cases but subject to a condition like expression (38). This also means that pressure drop reduction does not constitute a criterion to demonstrate experimentally the existence of slip. Indeed a more elevated pressure drop compared to nonslip flow could paradoxically be explained by slip occurrence. Table 3 summarizes the conditions under which some experimental works were conducted and the values of slip lengths l_s reported. The slip rate w and the depression ΔP_σ caused inside the capillary are calculated using Eqs. A7 and 14, respectively. For rectangular channels,[4,8,48] Eqs. C4 and C6 are used. Values of ΔP_σ gives some idea of the magnitude of $\Delta P_\sigma^\varepsilon$ and by comparing to the measured pressure drop ΔP^ε one may judge if ignoring $\Delta P_\sigma^\varepsilon$ is acceptable or might lead to a strong underestimation of the slip. Exact values of $\Delta P_\sigma^\varepsilon$ cannot be calculated because there is no means to quantify the slip reversibility from the data. On the other hand, elevated values of ΔP_σ may indicate if cavitation is likely to occur. In the work of Churaev et al.,[7] ΔP_σ is small compared with ΔP^ε and L/R values are large so that ΔP^ε is practically dominated by viscous dissipation while entrance and exit effects (including the possible slip irreversibility) may be ignored; the reported l_s are then likely to be close to the actual values. Similar comments may be done about Ulmanella and Ho's[4] experiments. Pfahler et al.[8] observed that ΔP^ε was significantly greater than predicted with classical theory (corresponding to $\Delta P_{\mu 0}$). Although no information about slip was given, the calculated value of ΔP_σ (considering a maximum slip, $w = 1$) shows that slip irreversibility may affect significantly the total pressure drop and this could explain the unexpected behavior reported by the authors. Regarding Cheng and Giordano's[48] experiments, the slip causes a strong depression that highly exceeds the measured pressure drop. Because the liquid exits at atmospheric pressure according to the information given in

Table 3. Published Results of Experiments Involving Capillary Flows

Authors	Liquid/Solid	R or H (μm)	L/R or L/H	l_s (μm)	ΔP^ε (Pa)	w*	$\Delta P_\sigma^\dagger$ (Pa)
Churaev et al.[7]	Water/quartz	0.88	65,000	30×10^5	-30×10^5	0.12	-0.20×10^5
	Mercury/quartz	1.00	97,600	70×10^5	-50×10^5	0.22	-2.11×10^5
Ulmanella and Ho[4]	Isopropanol/silicon	1.37‡	>1000	30×10^{-3}	-20×10^5	0.12	-0.03×10^5
	Hexadecane/silicon	0.35‡	>1000	120×10^{-3}	-20×10^5	0.67	-1.03×10^5
Pfahler et al.[8]	Propanol/silicon	0.79‡	/	/	-1.4×10^5 to -4×10^5	/	-0.59×10^5§
Cheng and Giordano[48]	Hexadecane/photoresist	0.05‡	>2000	25×10^{-3}	-1.2×10^5	0.75	-8.10×10^5
Holt et al.[18]	Water/polycarbonate	0.008	750	5×10^{-3}	/	0.63	-113.4×10^5
Cheikh and Koper[12]	Water + surfactant/ polycarbonate	0.05	200	20×10^{-3}	-1.5×10^5	0.62	$> -17.8 \times 10^5$
Hasegawa et al.[19]	Water/Harver	4.4	2.28	/	-0.06×10^5 to -0.18×10^5	/	-0.33×10^5§

Slip lengths l_s are inferred by considering the measured (total) pressure drop ΔP^ε only caused by viscous dissipation. In general, ΔP^ε may include others effects like irreversible slip variation and cavitation (see comments in the text).
*Calculated from Eqs. A7 and C4.
†Based on σ_{lv}, Eqs. 14 and C6.
‡Channel height H ($\approx$ hydraulic radius R_H, see Appendix C).
§Maximum value ($w = 1$).

that paper, the driving pressure is about 2.2×10^5 Pa; the value of ΔP_σ shows that the occurrence of a vapor phase and even cavitation are highly probable. Thus, modeling ΔP^ε simply as the pressure drop of a liquid phase may be questionable. As discussed earlier, adopting such hypothesis may result in an overestimation of ΔP_μ and the calculated l_s is probably lower that the actual value. The same remarks could be done regarding the investigation of Holt et al.[18] and Cheikh and Koper,[12] who considered membranes of nanometric pore size. The work of Hasegawa et al.[19] concerns orifices, the authors measured a pressure drop 3 times greater than predicted with classical hydrodynamics, noting that due to small value of L/R entrance and exit effects are dominant. Considering the conditions under which Hasegawa et al. performed their experiments, the results probably involve slip irreversibility effects. The authors dismissed the slip as a possible cause invoking the general opinion according to which it rather reduces the pressure drop.[49] As analyzed above, this is not always true because slip irreversibility and slip cavitation when occurring may have an opposite effect.

Conclusions

The matter presented in this work is a contribution to the application of thermodynamics fundamentals to capillary flows showing hydrodynamic slip at the boundary. The thermodynamic approach reveals valuable information concerning the general behavior of such a system. The study of different types of capillary flows was undertaken with the possibility to derive heat-transfer, pressure, and temperature change during the flow. An extended form of Bernoulli's equation including slip effects has been derived permitting a simple comparison with conventional flows. Capillary effects are involved because in the presence of slip there is a transfer of molecules from the boundary to the bulk and vice versa. This process is a thermodynamic transformation that may present an irreversible character. Slip development in a capillary increases the specific area of interface and thus leads to a decrease in pressure. This effect may cause degassing of dissolved gases, vaporization, and ultimately cavitation. The analysis presented shows that slip does reduce viscous dissipation but at the same time may cause additional pressure drop if the slip is irreversible and if cavitation takes place inside the capillary. The results derived in this work result from a theoretical analysis leaning on thermodynamics; some published experimental results based on the pressure drop method were commented from the point of view considered in this work. To confirm in a more evident manner the effects described, there is a need for experimental investigations specifically dedicated to this goal. The subject of these experiments could be the measurement of the pressure distribution inside a capillary or a channel to observe the depression caused by the slip and to infer its magnitude, the detection of cavitation inside the capillary, the study of the slip reversibility as a function of the capillary shape.

Acknowledgments

This work is part of the project research N° J0101720060017 registered by the Comité National d'Evaluation et de Programmation de la Recherche Universitaire—CNEPRU. The authors acknowledge Mr. Farid Berrahil and Mr. Omar Laghrouche for bibliographic research assistance.

Notation

A = surface area (m^2)
a = specific surface area ($m^2\ kg^{-1}$)
c_v = heat capacity ($J\ kg^{-1}\ K^{-1}$)
D = channel width (m)
e_c, e_p = specific kinetic, potential energy ($J\ kg^{-1}$)
f = parietal friction coefficient ($Pa\ s\ m^{-1}$)
g = gravity acceleration ($m\ s^{-2}$)
H = channel height (m)
h = enthalpy per kg or m^2 ($J\ kg^{-1}$, $J\ m^{-2}$)
l_s = slip length (m)
L = length of capillary or channel (m)
$\dot{m}$ = mass flow rate ($kg\ s^{-1}$)
M = molar mass ($g\ mol^{-1}$)
P = pressure (Pa)
Q, $\dot{Q}$ = heat per kg, heat-transfer rate ($J\ kg^{-1}$, W)
r = radial coordinate (m)
R = capillary radius (m)
R_{id} = ideal gas constant ($8.314\ J\ mol^{-1}\ K^{-1}$)
s = entropy per kg or m^2 ($J\ kg^{-1}\ K^{-1}$, $J\ m^{-2}\ K^{-1}$)
T = temperature (K)
t = time (s)
u = internal energy per kg or m^2 ($J\ kg^{-1}$, $J\ m^{-2}$)
v = specific volume ($m^3\ kg^{-1}$)
$\dot{v}$ = volume flow rate ($m^3\ s^{-1}$)
V = velocity ($m\ s^{-1}$)
w = slip rate
$\dot{W}$ = power (W)
x = longitudinal coordinate (m)
z = elevation (m)

Greek letters

ε,$\dot{\varepsilon}$ = entropy generation ($J\ kg^{-1}\ K^{-1}$, $W\ K^{-1}$)
μ = dynamic viscosity (Pa s)
η = thermodynamic efficiency
ρ = density ($kg\ m^{-3}$)
σ = surface tension ($J\ m^{-2}$)
θ = contact angle (rad)

Superscripts

sat = saturation state
ε = related to an irreversible process

Subscripts

b = boundary
c = related to the cross section
g = overall thermodynamic property
H = hydraulic (radius)
l = liquid
r = quantity function of radius
s = related to slip
V = related to flow velocity
Z = related to elevation
lv = liquid–vapor surface
sl = solid–liquid interface
sv = solid–vapor interface
gap = gas or vapor gap
0 = for noncurved surface or conditions at $r = 0$
μ = related to viscous dissipation
σ = related to surface effects

Literature Cited

1. Joseph P. Etude expérimentale du glissement sur surface lisses et textures. PhD Thesis. University Paris 6: France, 2005.

2. Rothstein JP. Slip on superhydrophobic surfaces. *Annu Rev Fluid Mech*. 2010;42:89–109.
3. Laouir A, Luo L, Tondeur D, Cachot T, LeGoff P. Thermal machines based on surface energy of wetting thermodynamic analysis. *AIChE J*. 2003;49:764–781.
4. Ulmanella U, Ho CM. Molecular effects on boundary condition in micro/nanoliquid flows. *Phys Fluids*. 2008;20:101512-1–101512-9.
5. Lauga E, Brenner MP, Stone HA. *Microfluidics: the no-slip boundary condition*. In: Tropea C, Yarin A, Foss JF, editors. *Handbook of Experimental Fluid Dynamics*. New York: Springer, 2007:1218–1240.
6. Papautsky I, Ameel T, Frazier AB. *A review of laminar single-phase flow in microchannels*. In: *Proceedings of 2001 ASME International Mechanical Engineering Conference and Exposition*, November, New York, 2001:1–9.
7. Churaev NV, Sobolev VD, Somov AN. Slippage of liquids over lyophobic solid surfaces. *J Colloid Interface Sci*. 1984;97:574–581.
8. Pfahler J, Harley J, Bau H, Zemel J. Liquid transport in micron and submicron channels. *Sens Actuators*. 1990; A21–A23:431–434.
9. Mala GhM, Li D. Flow characteristics of water in microtubes. *Int J Heat Fluid Flow*. 1999;20:142–148.
10. Weilin Qu, Mala GhM, Li D. Pressure-driven water flows in trapezoidal silicon microchannels. *Int J Heat Mass Transf*. 2000;43:353–364.
11. Choi HC, Westin KJA, Breuer KS. *To slip or not to slip water flows in hydrophilic and hydrophobic microchannels*. In: *Proceedings of 2002 ASME International Mechanical Engineering Conference and Exposition*, November, New Orleans, 2002:1–8.
12. Cheikh C, Koper G. Stick-slip transition at the nanometer scale. *Phys Rev Lett*. 2003;91:156102-1–156102-4.
13. Sinha S, Rossi MP, Mattia D, Gogotsi Y, Bau HH. Induction and measurement of minute flow rates through nanopipes. *Phys Fluids*. 2007;19:013603-1–013603-8.
14. Cottin-Bizonne C, Jurine S, Baudry J, Crassous J, Restagno F, Charlaix E. Nanorheology: an investigation of the boundary condition at hydrophobic and hydrophilic interfaces. *Eur Phys J E*. 2002;9:47–53.
15. Craig VSJ, Neto C, Williams DRM. Shear-dependent boundary slip in an aqueous Newtonian liquid. *Phys Rev Lett*. 2001;87:054504-1–054504-4.
16. Tretheway DC, Meinhart CD. Apparent fluid slip at hydrophobic microchannel walls. *Phys Fluids*. 2002;14:9–12.
17. Verweij H, Schillo MC, Li J. Fast mass transport through carbon nanotube membranes. *Small*. 2007;3:1996–2004.
18. Holt JK, Park HG, Wang Y, Stadermann M, Artyukhin AB, Grigoropoulos CP, Noy A, Bakajin O. Fast mass transport through sub-2-nanometer carbon nanotubes. *Science*. 2006;312:1034–1037.
19. Hasegawa T, Suganuma M, Watanabe H. Anomaly of excess pressure drops of the flow through very small orifices. *Phys Fluids*. 1997; 9:1–3.
20. de Gennes PG. Wetting: statics and dynamics. *Rev Mod Phys*. 1985; 57:828–861.
21. Vinogradova OI. Slippage of water over hydrophobic surfaces. *Int J Miner Process*. 1999;56:31–60.
22. Tabling P. Phénomènes de glissement à l'interface liquide-solide. *C R Phys*. 2004;5:531–537.
23. Tretheway DC, Meinhart CD. A generating mechanism for apparent fluid slip in hydrophobic microchannels. *Phys Fluids*. 2004;16:1509–1515.
24. Huang DM, Sendner C, Horinek D, Netz RR, Bocquet L. Water slippage versus contact angle: a quasiuniversal relationship. *Phys Rev Lett*. 2008;101:226101-1–226101-4.
25. Priezjev NV. Rate-dependent slip boundary conditions for simple fluids. *Phys Rev E*. 2007;75:051605-1–051605-7.
26. Ellis JS, McHale G, Hayward GL, Thompson M. Contact angle-based predictive model for slip at the solid-liquid interface of a transverse-shear mode acoustic wave device. *J Appl Phys*. 2003; 94:6201–6207.
27. Sun G, Bonaccurso E, Franz V, Butt HJ. Confined liquid: simultaneous observation of a molecularly layered structure and hydrodynamic slip. *J Chem Phys*. 2002;117:10311–10314.
28. Barrat JL, Bocquet L. Influence of wetting properties on hydrodynamic boundary conditions at a fluid/solid interface. *Faraday Discuss*. 1999;112:119–127.
29. Moelwyn-Hughes EA. *Physical Chemistry*. London: Pergamon Press, 1951.
30. Adamson AW. *Physical Chemistry of Surfaces*. New York: Interscience Publishers, 1960.
31. Defay R, Prigogine I. *Tension Superficielle et Adsorption*. Paris: Dunod, 1951.
32. Harkins WD, Jura G. An absolute method for the determination of the area of a finely divided crystalline solid. *J Am Chem Soc*. 1944;66:1362–1373.
33. Melrose JC. On the thermodynamic relations between immersional and adhesional wetting. *J Colloid Sci*. 1965;20:801–821.
34. Zisman WA. *Relation of the equilibrium contact angle to liquid and solid constitution*. In: Gould RF, editor. *Contact angle wettability and adhesion. Advances in Chemistry Series* 43. Washington, D.C.: American Chemical Society, 1964:1–51.
35. Churaev NV, Sobolev VD. Wetting of low-energy surfaces. *Adv Colloid Interfaces Sci*. 2007;15:15–23.
36. Neumann AW. Contact angles and their temperature dependence. *Adv Colloid Interfaces Sci*. 1974;4:105–168.
37. Kwok DY, Neumann AW. Contact angle interpretation in terms of solid surface tension. *Colloids Surf A*. 2000;161:31–48.
38. Laouir A, Tondeur D. *Thermodynamic aspects of capillary flows*. In: *Proceedings of International Conference on Micro and Nano Technologies (ICMNT'06)*, November, Tizi-Ouzou, Algeria, 2006: 35–36.
39. Laouir A, Tondeur D. Some new results from applying thermodynamics to wetting phenomena. *Int J Thermodyn*. 2008;11:61–69.
40. Eroshenko V, Regis RC, Soulard M, Patarin J. Les systèmes hétérogènes eau-zéolithe hydrophobe: de nouveaux ressorts moléculaires. *C R Phys*. 2002;3:111–119.
41. Chen YT, Kang SW, Tuh WC, Hsiao TH. Experimental investigation of fluid flow and heat transfer in microchannels. *Tamkang J Sci Eng*. 2004;7:11–16.
42. Mishra C, Peles Y. Cavitation in flow through a micro-orifice inside a silicon microchannel. *Phys Fluids*. 2005;17:013601-1–013601-15.
43. Mishra C, Peles Y. An experimental investigation of hydrodynamic cavitation in micro-Venturis. *Phys Fluids*. 2006;18:103603-1–103603-5.
44. Janssens-Maenhout GGA, Schulenberg T. An alternative description of the interfacial energy of a liquid in contact with a solid. *J Colloid Interface Sci*. 2003;257:141–153.
45. Ren L, Qu W, Li D. Interfacial electrokinetic effects on liquid flow in microchannels. *Int J Heat Mass Transf*. 2001;44:3125–3134.
46. Öttinger HC. Thermodynamic formulation of wall slip. *J Non-Newtonian Fluid Mech*. 2008;152:66–75.
47. Spikes H, Granick S. Equation for slip of simple liquids at smooth solid surfaces. *Langmuir*. 2003;19:5065–5071.
48. Cheng JT, Giordano N. Fluid flow through nanometer-scale channels. *Phys Rev E*. 2002;65:031206-1–031206-5.
49. Hasegawa T, Watanabe H, Sato T, Watanabe T, Takahashi M, Narumi T, Tiu C. Anomalous reduction in thrust/reaction of water jets issuing from microapertures. *Phys Fluids*. 2007;19:053102-1–053102-8.

Appendix A: Laminar Slip Flow in a Cylindrical Duct

The flow of a liquid in a cylindrical duct is governed by 1-D Navier-Stokes equation, the later expresses the equilibrium of a section of fluid of length L and radius r:

$$\text{Pressure forces } (P_1 - P_2)\pi r^2 + \text{Viscous shear forces } \mu \frac{dV_r}{dr} 2\pi r L = 0 \quad \text{(A1)}$$

The integration of relation (A1) allows to determine the velocity profile and to derive the expression relating the

pressure drop caused by viscosity $\Delta P_\mu = -(P_1 - P_2)$ to the flow parameters. The pressure drop ΔP_μ is a result of all friction forces acting between $r = 0$ and $r = R$ (including the two limits). Therefore, in presence of slip, wall-friction force $\mu(dV_r/dr)_R 2\pi RL$ contribution to the pressure drop is naturally included in ΔP_μ expression that will be derived. Letting $c = -\Delta P_\mu/(4\mu L)$ and having the condition $V_r(r = 0) = V_0$, the integration of relation (A1) gives,

$$V_r = V_0 - cr^2 \tag{A2}$$

having also $V_r(r = R) = V_s$, Eq. A2 gives $V_0 = V_s + cR^2$, and substituting in Eq. A2,

$$V_r = V_s + c(R^2 - r^2) \tag{A3}$$

The slip length is defined by Eq. 1 so,

$$l_s = \frac{V_s}{2cR} \tag{A4}$$

The average speed defined as the ratio of the volumetric flow rate to the cross section area is,

$$V = \frac{\int_0^R V_r 2\pi r dr}{\pi R^2} = V_s + \frac{1}{2}cR^2 \tag{A5}$$

The volume flow rate is $\dot{v} = (V_s + 1/2cR^2)\pi R^2$.

Substituting c by its expression in Eq. A5 and resolving for ΔP_μ,

$$\Delta P_\mu = -8\mu L(V - V_s)/R^2 \tag{A6}$$

the slip rate $w = V_s/V$ may be expressed as a function of the ratio l_s/R; from Eqs. A4 and A5,

$$w = \frac{l_s/R}{l_s/R + 1/4} \tag{A7}$$

All the relations written above are valid for the nonslip case by setting $V_s = 0$ or $w = 0$. The flow rate with non-slip condition is $\dot{v}_0 = (1/2cR^2)\pi R^2$, therefore

$$\frac{\dot{v}}{\dot{v}_0} = 1 + 4\frac{l_s}{R} = \frac{1}{1 - w} \tag{A8}$$

Appendix B: Occurrence of Saturation State at the Boundary

In the Reversible and Isothermal Flow section, a discussion about saturation state occurrence at the interface was addressed for nonviscous flow. The discussion is completed in this appendix by considering the more realistic case of a viscous fluid. Supposing that slip develops reversibly at the capillary entrance, we write in general,

$$P_2 - P_1 = \Delta P_\sigma + \Delta P_\mu \tag{B1}$$

Taking into account Eq. 17, Eq. B1 becomes:

$$P_{\text{gap}} = P_1 - \frac{2\sigma_{\text{lv}}}{R}(1 + w) - 8\mu LV(1 - w)/R^2 \tag{B2}$$

By setting $P_{gap} = P^{\text{sat}}(T,R)$ given by Eq. 18, relation (B2) allows calculating the length L^{sat} at which the saturation pressure at the boundary is reached,

$$L^{\text{sat}} = \frac{R(P_1 - P^{\text{sat}}) - 2\sigma_{\text{lv}}(1 + w)}{8\mu V(1 - w)/R} \tag{B3}$$

The driving pressure P_1 may be expressed as a function of the total pressure drop between the two ends $P_1 = P_3 - \Delta P^\varepsilon$, where P_3 is the exit pressure generally equal to atmospheric pressure. If the flow is completely free from slip irreversibility and cavitation, one may write $\Delta P^\varepsilon = \Delta P_\mu = -8\mu LV(1 - w)/R^2$. The slip rate w is rather an average value here because slip conditions may locally change. Substituting into Eq. B3, we finally obtain

$$\frac{L^{\text{sat}}}{L} \approx 1 - \left[P_3 - P^{\text{sat}} - \frac{2\sigma_{\text{lv}}}{R}(1 + w)\right] \Big/ \Delta P^\varepsilon \tag{B4}$$

Appendix C: Relations for Slip Flow in a Channel of Rectangular Cross Section

The channel has a height H, a width D, and a length L, generally $D \gg H$ so as the flow may be modeled as one-dimensional flow between two infinite plates.[1,11,48] The following relations may be derived, the slip length is,

$$l_s = \frac{V_s}{2cH} \tag{C1}$$

where $c = -\Delta P_\mu/(4\mu L)$, the mean flow velocity is given by,

$$V = V_s + \frac{1}{3}cH^2 \tag{C2}$$

the viscous pressure drop is then,

$$\Delta P_\mu = -12\mu L(V - V_s)/H^2 \tag{C3}$$

From Eqs. C1 and C2, the slip rate w expression is,

$$w = \frac{l_s/H}{l_s/H + 1/6} \tag{C4}$$

the flow rate is $\dot{v} = (V_s + cH^2/3)HD$, in the absence of slip ($V_s = 0$) $\dot{v}_0 = HDcH^2/3$ so,

$$\frac{\dot{v}}{\dot{v}_0} = 1 + 6\frac{l_s}{H} = \frac{1}{1 - w} \tag{C5}$$

With the assumption $D >> H$, the hydraulic radius is practically equal to the channel height: $R_H = 2HD/2(H + D) \approx$

H. The specific area of slip is then $a = 2w/(\rho R_H) \approx 2w/(\rho H)$ and the capillary pressure of slip,

$$\Delta P_\sigma \approx -\frac{2w}{H}\sigma_{\mathrm{b}}(T) \tag{C6}$$

Unlike in small size circular capillaries, the boundary with rectangular channels is not curved, so the pressure in the gas gap, when it exists, is equal to that in the liquid ($P_{gap} = P_2$) and the vapor tension of the fluid is not increased ($P_{gap} = P_0^{\mathrm{sat}}$).

$$P_2 - P_1 = P_0^{\mathrm{sat}} - P_1 = \Delta P_\sigma + \Delta P_\mu \tag{C7}$$

the length at which the saturation state is reached is then,

$$L^{\mathrm{sat}} = \frac{H\left(P_1 - P_0^{\mathrm{sat}}\right) - 2w\sigma_{\mathrm{lv}}}{12\mu V(1-w)/H} \tag{C8}$$

The friction coefficient f like for circular capillaries is related to viscosity and slip length by the relation $f = \mu/l_s$ and from Eq. C4 $l_s = Hw/6(1-w)$ so,

$$f = \frac{6\mu(1-w)}{wH} \tag{C9}$$

Manuscript received Apr. 10, 2010, and revision received Aug. 21, 2010.